Effects of Ionic Strength and Surface Charge on Protein Adsorption at PEGylated Surfaces

Stéphanie Pasche,*,†,‡ Janos Vörös,† Hans J. Griesser,‡ Nicholas D. Spencer,† and Marcus Textor†

BioInterfaceGroup, Laboratory for Surface Science and Technology, Department of Materials, Swiss Federal Institute of Technology (ETH) Zurich, CH-8093 Zurich, Switzerland, and Ian Wark Research Institute, University of South Australia, Mawson Lakes, SA 5095, Australia

Received: January 25, 2005; In Final Form: May 17, 2005

PEGylated Nb_2O_5 surfaces were obtained by the adsorption of poly(L-lysine)-*g*-poly(ethylene glycol) (PLL-*g*-PEG) copolymers, allowing control of the PEG surface density, as well as the surface charge. PEG (MW 2 kDa) surface densities between 0 and 0.5 nm^{-2} were obtained by changing the PEG to lysine-mer ratio in the PLL-*g*-PEG polymer, resulting in net positive, negative and neutral surfaces. Colloid probe atomic force microscopy (AFM) was used to characterize the interfacial forces associated with the different surfaces. The AFM force analysis revealed interplay between electrical double layer and steric interactions, thus providing information on the surface charge and on the PEG layer thickness as a function of copolymer architecture. Adsorption of the model proteins lysozyme, α-lactalbumin, and myoglobin onto the various PEGylated surfaces was performed to investigate the effect of protein charge. In addition, adsorption experiments were performed over a range of ionic strengths, to study the role of electrostatic forces between surface charges and proteins acting through the PEG layer. The adsorbed mass of protein, measured by optical waveguide lightmode spectroscopy (OWLS), was shown to depend on a combination of surface charge, protein charge, PEG thickness, and grafting density. At high grafting density and high ionic strength, the steric barrier properties of PEG determine the net interfacial force. At low ionic strength, however, the electrical double layer thickness exceeds the thickness of the PEG layer, and surface charges "shining through" the PEG layer contribute to protein interactions with PLL-*g*-PEG coated surfaces. The combination of AFM surface force measurements and protein adsorption experiments provides insights into the interfacial forces associated with various PEGylated surfaces and the mechanisms of protein resistance.

1. Introduction

Spontaneous adsorption of proteins from biological fluids onto synthetic materials such as biomaterials and biomedical devices may induce undesirable reactions of the body to the foreign materials, such as immune responses, blood coagulation, or bacterial adhesion.[1,2] In the bioaffinity sensor field, suppression of nonspecific protein adsorption is crucial for achieving sufficient bioassay selectivity and sensitivity.[3] Elimination of protein adsorption requires the suppression of all attractive forces between proteins and the surface. Studies investigating the driving forces for protein adsorption have demonstrated the importance of enthalpic contributions, such as van der Waals, electrical double layer, and hydrophobic interactions. At the same time, entropically based mechanisms entail the release of counterions and/or solvation water, and the reduction of ordered structure due to adsorption-induced conformational changes.[4−6] Due to the diversity of the interactions between proteins and surfaces, a preferred strategy for blocking the adsorption of proteins is to immobilize polymers in the form of well-solvated brushes (e.g., poly(ethylene glycol), PEG) on the surface. The polymer layer shields the surface, introducing a high activation barrier for the proteins to adsorb.[7]

The ability of polymer brushes to prevent the adsorption of proteins has been addressed theoretically, showing the importance of chain length and density.[8−12] Three modes of adsorption have been proposed: (i) primary adsorption due to proteins diffusing through the interfacial region to the underlying substrate and adsorbing onto the substrate (invasive mechanism); (ii) secondary adsorption at the outer surface of the brush due to protein-brush interactions; (iii) adsorption of proteins upon compression of the polymer film (compressive mechanism).[12] Protein resistance requires the exclusion of all three processes. The thickness of the grafted PEG layer must be sufficient to screen protein−substrate interactions, and the brush chain density must be high enough to block diffusion through this steric layer.

Poly(ethylene glycol) (PEG) has been shown to successfully confer protein resistance to a variety of surfaces.[13,14] Both PEG chain length and surface coverage have been demonstrated to play a key role in imparting protein resistance, with PEG chains of typically 1−10 kDa molecular weight providing protein resistance, provided that the chain density is sufficiently high, hence indicating the need for a high surface density of ethylene glycol monomer units.[7,15−20] Short, densely packed oligo-$(EG)_{2-7}$-terminated alkanethiol self-assembled monolayers on gold have also been shown to confer protein resistance to surfaces.[21−23] While there remains no general agreement, the protein resistance by PEG chains has been associated with two main mechanisms, steric repulsion and a hydration or water-structuring layer.[13,14]

* To whom correspondence should be addressed. Present address: Centre Suisse d'Electronique et de Microtechnique SA (CSEM), Jaquet-Droz 1, CH-2007 Neuchâtal. E-mail: stephanie.pasche@csem.ch. Telephone: +41-32-7205540. Fax: +41-32-7205740.

† Swiss Federal Institute of Technology (ETH) Zurich.

‡ University of South Australia.

10.1021/jp050431+ CCC: $30.25
Published on Web 08/24/2005

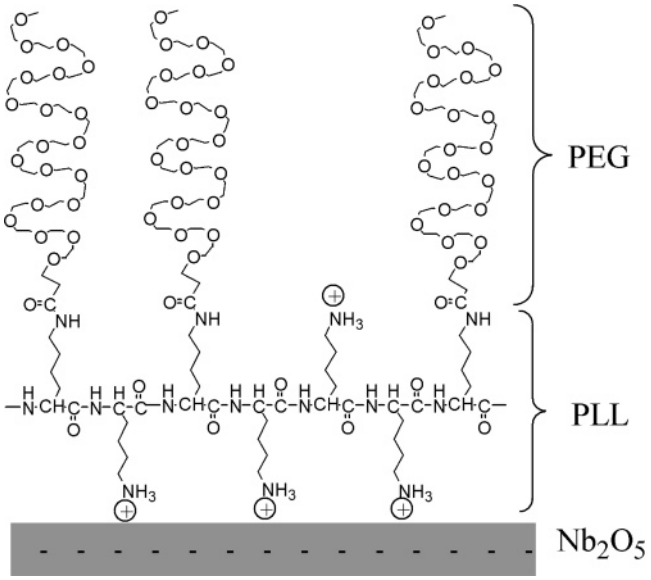

Figure 1. Idealized scheme of the interfacial structure of a monolayer of PLL-*g*-PEG adsorbed on a metal oxide substrate (Nb_2O_5) via electrostatic interactions between the negatively charged metal oxide substrate and positively charged amino-terminated PLL side chains (at neutral pH).

Self-organized monolayers of PEG-grafted polyelectrolytes such as poly(L-lysine)-*g*-poly(ethylene glycol) (PLL-*g*-PEG) have been shown to provide a means of quantitative control of PEG surface coverage, with the adsorbed protein (serum) mass correlating directly with the surface density of ethylene glycol monomer units.[20,24,25] PLL-*g*-PEG is a polycationic copolymer with PEG chains covalently grafted onto a positively charged (at neutral pH) PLL backbone. The copolymer spontaneously adsorbs from aqueous solution via electrostatic interactions onto negatively charged surfaces such as SiO_2, TiO_2, TCPS, and Nb_2O_5 (Figure 1).[26]

This study aims at an improved understanding of the mechanisms of protein resistance of PEG layers, using the comb-graft-copolymer poly(L-lysine)-*g*-poly(ethylene glycol) (PLL-*g*-PEG), and concerns the effects of systematic variations in the surface properties, in particular PEG chain length and density, and surface charge. PLL-*g*-PEG is used as a tool to decouple the different contributions to protein-surface interactions, by allowing surface charge and PEG surface density to be independently varied. Five surfaces with different surface charges and PEG surface densities have been analyzed by recording force−distance curves with the colloid probe atomic force microscope (AFM) at different ionic strengths, thus enabling identification and detailed analysis of the electrical double layer and steric repulsion contributions to the total interfacial force on each of the various PLL-*g*-PEG coated surfaces.[27] To elucidate how these interfacial forces and their relative magnitudes affect the adsorption of proteins, the results of the colloid probe AFM study are correlated with the adsorbed mass of three model proteins, lysozyme, myoglobin, and α-lactalbumin in buffers of different ionic strength, as measured by optical waveguide lightmode spectroscopy (OWLS). The proteins are selected on the basis of their similarity in size and structure, while showing variations in their net charge (Table 1).[28]

2. Materials and Methods

2.1. Materials. PLL-*g*-PEG polymers were synthesized from a stoichiometric mixture of poly(L-lysine) hydrobromide (PLL) (Sigma, USA, MW 15−30 kDa, polydispersity 1.3) and a *N*-hydroxysuccinimidyl ester of methoxy-terminated poly(ethylene glycol) (mPEG-SPA) (Nektar, USA, MW 2 kDa, polydispersity <1.05). The notation used for PLL(*x*)-*g*[*y*]-PEG(*z*) copolymers indicates the average molecular weights (MWs) of PLL-HBr (*x*) and PEG (*z*), and the grafting ratio, *g* (*y*). The grafting ratio, expressed as the number of lysine monomers divided by the number of PEG side chains (Lys/PEG ratio), was determined by ^{1}H NMR. The synthesis and characterization have been described elsewhere.[20]

Lysozyme from chicken egg white, myoglobin from horse heart, and α-lactalbumin from bovine milk (Sigma, Buchs, Switzerland) were used as model proteins for the protein adsorption assays. Lysozyme (LSZ), an enzyme (hydrolase) that attacks the protective cell walls of bacteria, myoglobin (MGB), an oxygen-binding haem protein active in the storage and transport of oxygen, and α-lactalbumin (α-LA), a calcium-binding protein involved in lactogenesis, are globular proteins with similar sizes and molecular weights, but different net charge (see Table 1).[29] At pH 7.4, lysozyme is positively charged, myoglobin neutral, and α-lactalbumin negatively charged. Protein solutions were obtained by dissolving the protein in buffer at a concentration of 0.5 mg/mL.

Adsorption of PLL-*g*-PEG as well as all in situ experiments and protein studies was conducted in a 4-(2-hydroxyethyl)-piperazine-1-ethane-sulfonic acid- (HEPES-) based buffer (Fluka, Buchs, Switzerland) adjusted to pH 7.4 with NaOH 6 M (Fluka, Buchs, Switzerland). The choice of the buffer system is important for the type of studies performed in this work: While phosphate-containing buffers result in strong binding of phosphate to transition metal cations and therefore change the surface properties in a time-dependent manner, HEPES is a buffer system with only weak interaction with metal oxide surfaces. The ionic strength of the buffer varied between 1 and 160 mM, either by dilution or by addition of NaCl (Fluka, Buchs, Switzerland). The following buffers were prepared: 1

TABLE 1: Selected Physical Properties of the Proteins Lysozyme (LSZ), Myoglobin (MGB), and a-Lactalbumin (α-LA) Investigated in This Study[28]

property	LSZ	MGB	α-LA
molar mass [g·mol^{-1}]	14 600	17 800	14 200
partial specific vol [cm^3·g^{-1}]	0.688	0.742	0.735
dimensions [nm^3]	4.5 × 3.0 × 3.0	4.5 × 3.5 × 2.5	3.7 × 3.2 × 2.5
diffusion coeff [m^2·s^{-1}]	1.04·10^{-10}	1.10·10^{-10}	1.06·10^{-10}
isoelectric point [pH units]	11.1	7.0	4.3
no. of net charges at pH 7.4	+ 6.8	+ 0.6	- 11.2
overall hydrophobicity [J·g^{-1}]	−7.6	−4.1	−5.8
Gibbs energy of denaturation [J·g^{-1}][a]	−4.1	−2.8	−1.5
secondary structure			
percentage α-helix	42	75	26
percentage *β*-sheet			14

[a] Heat denaturation.

mM HEPES (H0), 10 mM HEPES (H1), and 150 mM NaCl in 10 mM HEPES (H2). Ultrapure Millipore water (organic content less than 5 ppb) was used for the preparation of all buffers and experiments.

2.2. Substrates. PLL-*g*-PEG was used to modify the surface of niobium oxide films. 12 nm thick films of Nb_2O_5 were sputter coated onto silicon wafers ⟨110⟩ (WaferNet GmbH, Eching, Germany) using reactive magnetron sputtering (PSI, Villigen, Switzerland) to produce substrates for the AFM measurements. Optical waveguide chips for OWLS measurements (Microvacuum Ltd., Budapest, Hungary) consisted of a 1 mm-thick AF45 glass substrate and a 200 nm-thick $Si_{0.75}Ti_{0.25}O_2$ waveguiding surface layer, with a total size of 1.2 × 0.8 cm. A 12 nm-thick Nb_2O_5 layer was sputter-coated on top of the waveguiding layer under the same deposition conditions as described above for the silicon wafers. Niobia was used as the substrate surface in view of its high negative charge density at neutral pH; in comparison to SiO_2, niobia surfaces proved to result in improved adlayer stability and consistency of the results.

The substrates used for AFM measurements were sonicated in 2-propanol for 10 min, rinsed with ultrapure water, dried under a nitrogen stream, followed by 2 min of oxygen-plasma cleaning in a plasma cleaner/sterilizer PDC-32G instrument (Harrick, Ossining, NY). The optical waveguide chips used for OWLS were cleaned and regenerated by washing with "Cleaner" solution (Roche, Basel, Switzerland), followed by 10 min sonication in 0.1 M HCl, rinsed with ultrapure water, dried under a nitrogen stream and exposed to 2 min of oxygen plasma.

2.3. Surface Modification. For AFM measurements, the clean substrates were immediately transferred to a filtered 1 mg/mL solution of PLL-*g*-PEG in 10 mM HEPES buffer solution (pH 7.4). After 30 min of immersion, resulting in the formation of a monolayer of PLL-*g*-PEG, the modified samples were withdrawn, rinsed extensively with ultrapure water and dried under nitrogen.[20,30] Deliberate desorption of part of the polymer monolayer was obtained through 10 min immersion of the samples in 10 mM HEPES with 2.8 M NaCl (pH 7.4), followed by rinsing with ultrapure water and drying under nitrogen. This resulted in the formation of a fractional monolayer of the polymer film with approximately 57% of the surface covered by the copolymer. Samples were analyzed with AFM immediately after adsorption, to avoid any uncertainty due to storage.

The surface modification process was monitored in situ with OWLS (see section 2.5).

2.4. Colloid Probe Atomic Force Microscopy. Colloid probe atomic force microscopy (AFM) uses a microsphere as a probe for the quantitative measurement of surface forces.[31−35] The main advantage of using a microsphere instead of a sharp tip is the improved definition of the contact geometry and thus the ability to perform quantitative comparisons with theoretical models of interfacial forces.

A Nanoscope IIIA Multimode (Digital Instruments, Santa Barbara, CA) was used for the atomic force microscopy measurements. The AFM was operated in the force mode, with a scan rate of 1 Hz and a *z*-piezo total displacement of 500 nm. Both approach/extension and retraction force curves of the cantilever were recorded. The experiments were performed in liquid, using an open fluid cell and letting the system equilibrate for 30−60 min. All buffers were filtered through a 0.22 μm pore size filter.

Experiments were performed with silica sphere tips and both uncoated and polymer-coated Nb_2O_5 surfaces. Silica microspheres (4−5 μm diameter) (Bangs Laboratories, USA) were attached to V-shaped Si_3N_4 AFM cantilevers with a nominal spring constant of 0.12 N/m (Novascan Technologies, Ames, IA). Prior to the force measurements the cantilevers were cleaned for 30 min in a UV/ozone cleaner (UV/ clean, model 135500, Boekel Industries, Inc., Feasterville, PA). Further details are provided elsewhere.[27]

Raw data were converted from cantilever deflection and z-piezo position into force-vs-distance curves. The force was calculated with Hooke's law ($F = k\delta$), where k is the spring constant and δ the deflection of the cantilever, and normalized to the radius of the SiO_2 sphere, R, relating the force to the interaction energy (Derjaguin approximation).[36] A positive force was associated with repulsion, while a negative force indicated attraction between the sphere and the surface. The point of zero separation, experimentally not accessible for a soft surface, was defined as the onset of the linear-constant-compliance region, where the polymer layer becomes maximally compressed for a given cantilever.[37] Data analysis was conducted for the approach/extension part of the curve.[27]

2.5. Optical Waveguide Lightmode Spectroscopy. In optical waveguide lightmode spectroscopy, the adsorbed mass is calculated from the change of the refractive index in the vicinity of the surface upon adsorption of molecules from solution. This change is monitored by the grating-induced incoupling of laser light into the waveguiding substrate, generating an evanescent wave.[38−40] The adsorbed mass was calculated from the thickness and refractive index of the adlayer according to de Feijter's formula, with dn/dc values of 0.18, 0.139, and 0.135 cm^3/g for pure PLL, PLL(20)-*g*[3.5]-PEG(2) and PLL(20)-*g*[10.1]-PEG-(2) polymers, respectively, and 0.182 cm^3/g for the proteins.[20,41] The sensitivity limit of the OWLS technique is typically 1−2 ng/cm^2.

In situ polymer adsorption was studied using a flow-through cell with a volume of 16 μL. The solution was typically replaced every 10 min.[38] The cleaned Nb_2O_5-coated waveguides were inserted into the OWLS flow-through cell, and equilibrated by immersing in HEPES buffer (pH 7.4) for at least 10 h in order to obtain a stable baseline. Subsequently, the buffer was exchanged in situ against a filtered solution of PLL-*g*-PEG (1 mg/mL) in HEPES buffer. After 30 min exposure to the polymer solution, resulting in the formation of a complete monolayer, the sample was rinsed with the HEPES buffer solution for another 30 min. Polymer desorption was achieved after 10 min exposure of the polymer layer to 10 mM HEPES with 2.8 M NaCl (pH 7.4), and a subsequent rinse with buffer. Protein adsorption onto bare and PLL-*g*-PEG-coated OWLS chips was studied in situ after 1 h exposure to 0.5 mg/mL protein solution and a subsequent rinse with the same buffer for about 1 h.

3. Results and Discussion

3.1. Surfaces with Different Polymer Architectures. PLL and PLL-*g*-PEG copolymers with PLL MW of ∼20 kDa (MW of PLL-HBr), PEG MW of 2 kDa and grafting ratios g of 3.5 and 10.1 were used to modify the Nb_2O_5-coated substrates, allowing the surface charge to be varied from negative (bare Nb_2O_5) to positive (PLL-coated Nb_2O_5), and the PEG surface density from 0 to 0.5 chains/nm^2, as measured by OWLS (eq 1).[20] While the PEG surface density is controlled through the PEG grafting ratio in the PLL-*g*-PEG polymer and the adsorbed polymer mass, the surface charge is determined by both the charge of the Nb_2O_5 substrate surface and the number of free amine groups in the lysine present in the polymeric monolayer. Only the lysine side chains that are not bound to a PEG chain carry a positive charge, as illustrated in the scheme of PLL-*g*-PEG in Figure 1. The number of free amines, n_{amine}(free) can

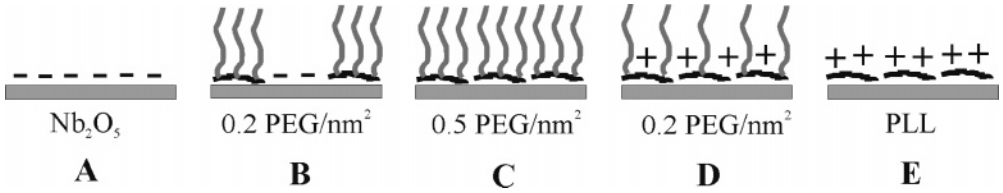

Figure 2. Surfaces used in the study that exhibit different surface charges and PEG surface densities: (A) bare niobium oxide substrate; (B) PLL(20)-*g*[3.5]-PEG(2)-coated Nb_2O_5 after partial desorption of the polymer layer with NaCl 2.8 M in 10 mM HEPES (half monolayer); (C) PLL(20)-*g*[3.5]-PEG(2)-coated Nb_2O_5 (full monolayer); (D) PLL(20)-*g*[10.1]-PEG(2)-coated Nb_2O_5 (monolayer); (E) PLL(20)-coated Nb_2O_5. The surface charge gradually changes from strongly negative (A) to strongly positive (E); the PEG surface density varies from 0 to a maximum of 0.5 chains per nm^2.

TABLE 2: Characteristics of the Surfaces Used for the Protein Adsorption Study: Surface Density of PEG Chains, n_{PEG}, and of Free Amine Groups in PLL, n_{amine}(free)[b], and "Surface Charge"

surface	n_{PEG} [nm^{-2}]	n_{amine}(free)[b] [nm^{-2}]	surface charge[c] [nm^{-2}]
Nb_2O_5	0		−1.30
PLL(20)	0	3.19 ± 0.52	+1.89
PLL(20)-*g*[10.1]-PEG(2)	0.27 ± 0.04	1.84 ± 0.28	+0.54
PLL(20)-*g*[3.5]-PEG(2)	0.51 ± 0.07	1.28 ± 0.17	−0.02
PLL(20)-*g*[3.5]-PEG(2) (1/2)[a]	0.22 ± 0.03	0.55 ± 0.08	−0.75

[a] (1/2) means that approximately half of the polymer monolayer has been desorbed by exposing the surface for 10 min to a 10 mM HEPES buffer solution with 2.8 M NaCl, leading to 57% desorption of the polymer (half monolayer coverage). [b] Amine groups of the lysine not bound to PEG chains and protonated at neutral pH. [c] Net "surface charge" calculated as the sum of the bare Nb_2O_5 surface charge (−1.30 nm^{-2}; see sections 3.1 and 3.2) and n_{amine}(free).

be calculated with eqs 1 and 2, where m_{pol} is the adsorbed polymer mass measured with OWLS [ng/cm^2], n_{Lys} and n_{PEG} are the numbers of adsorbed Lys monomers and PEG chains per nm^2, respectively, (eq 2), and g is the grafting ratio of the polymer, determined for the bulk polymer with ^{1}H NMR.[20]

$$n_{PEG} = \frac{m_{pol}}{M_{Lys}g + M_{PEG}} \quad (1)$$

$$n_{amine}(\text{free}) = n_{Lys}\left(1 - \frac{1}{g}\right) = n_{PEG}(g - 1) \quad (2)$$

Assuming that every free lysine side chain is protonated at pH 7.4 ($pK_a = 10.8$)[42] we can estimate the remaining surface charge, provided that the surface charge density of the Nb_2O_5 substrate is known. As this is not the case, the total surface charge of the bare Nb_2O_5 surface was estimated based on the AFM force curves (section 3.2). The AFM data for the PLL-(20)-*g*[3.5]-PEG(2)-coated Nb_2O_5 substrate indicated that the net surface charge sensed by the colloidal AFM tip was very close to zero (in fact, very slightly negative), implying that the negative surface charge of the bare niobia surface and the positive charges of the protonated amine groups in the adsorbed polymeric monolayer almost canceled each other out. Since the latter is known from NMR of the polymer and the OWLS adsorbed mass data to be 1.28 ± 0.17 nm^{-2} (eq 2), the surface charge of bare niobia was set to ∼−1.30 nm^{-2} (or 0.21 $C{\cdot}m^{-2}$), resulting in a very small negative surface charge for the PLL-(20)-*g*[3.5]-PEG(2)-coated Nb_2O_5 substrate, in agreement with the AFM information. Table 2 provides information on the surfaces used in this study, listing the PEG surface density, the number of ungrafted lysine-mers (i.e., non-PEGylated, protonated amine groups) per unit surface area, and the net surface charge estimated as discussed above.

As shown in Table 2, PLL(20)-*g*[3.5]-PEG(2) adsorption results in a nearly neutral surface with ∼0.5 PEG chains/nm^2, while PLL(20)-*g*[10.1]-PEG(2) shows a positive charge with ∼0.2 PEG chains/nm^2. To investigate the influence of the surface charge for a similar average PEG surface density, a negatively charged surface with ∼0.2 PEG/nm^2 was used. For this purpose, PLL(20)-*g*[3.5]-PEG(2) was adsorbed onto Nb_2O_5, and exposed to a 2.8 M NaCl in 10 mM HEPES buffer (pH 7.4) for 10 min, leading to 57% polymer desorption. As the resulting surface carries approximately half of a monolayer of PLL(20)-*g*-[3.5]-PEG(2), the notation "PLL(20)-*g*-[3.5]-PEG-(2) (1/2)" is used. Figure 2 illustrates the differences between the five surfaces used for the subsequent investigations, highlighting variations both in the PEG surface density and in the surface charge. The PLL-*g*-PEG technology therefore allows independent investigation of the influence of surface charge and PEG density on protein adsorption.

3.2. Surface Charge Measurement Using Colloid Probe AFM. Colloid probe AFM measurements were performed on all surfaces at different ionic strengths. The interaction between a 5 μm silica microsphere and the various surfaces contains both an electrostatic and a steric contribution to the total interfacial force; detailed analyses of the force curves including fits of the electrostatic forces to DLVO models are presented elsewhere.[27] While the electrostatic contribution provides information on the surface charge, the interplay with the steric force as a function of ionic strength demonstrated to what extent the PEG layer thickness is successful in screening the surface charge and eliminating the effects of the electrical double layer contribution beyond the uncompressed PEG layer, and it also provides an estimate for the hydrated thickness of the PEG layer.

Parts A−E of Figure 3 show the measured interfacial forces, normalized to the radius of the sphere, upon compression of the surface by the SiO_2 microsphere, plotted as a function of the apparent relative separation. The forces were measured at three ionic strengths, in 1 mM HEPES, 10 mM HEPES, and 10 mM HEPES with 150 mM NaCl buffer solutions (pH 7.4) (H0, H1, and H2), corresponding to Debye lengths of ∼10, ∼3, and <1 nm, respectively.[36]

The force between negatively charged silica and negatively charged niobia (Figure 3A) typically shows an electrostatic repulsion with a decay length increasing as the ionic strength decreases. Plotted on semilogarithmic axes (inset graph) the interactions at the three ionic strengths reflect the Debye lengths in the different solutions. Moving from A to E, the interaction gradually changes from repulsive to attractive, ending with a purely attractive interaction between the PLL-coated Nb_2O_5 and the silica microsphere. The data reflect the influence of the ionic strength and are characteristic of an electrical double layer force. As an attraction is associated with a negative force, the plots of Figure 3D,E are not shown on a semilogarithmic scale.

While the influence of the ionic strength probes the electrostatic nature of the interaction for the uncoated and PLL-coated Nb_2O_5 samples, it also provides relevant information for the

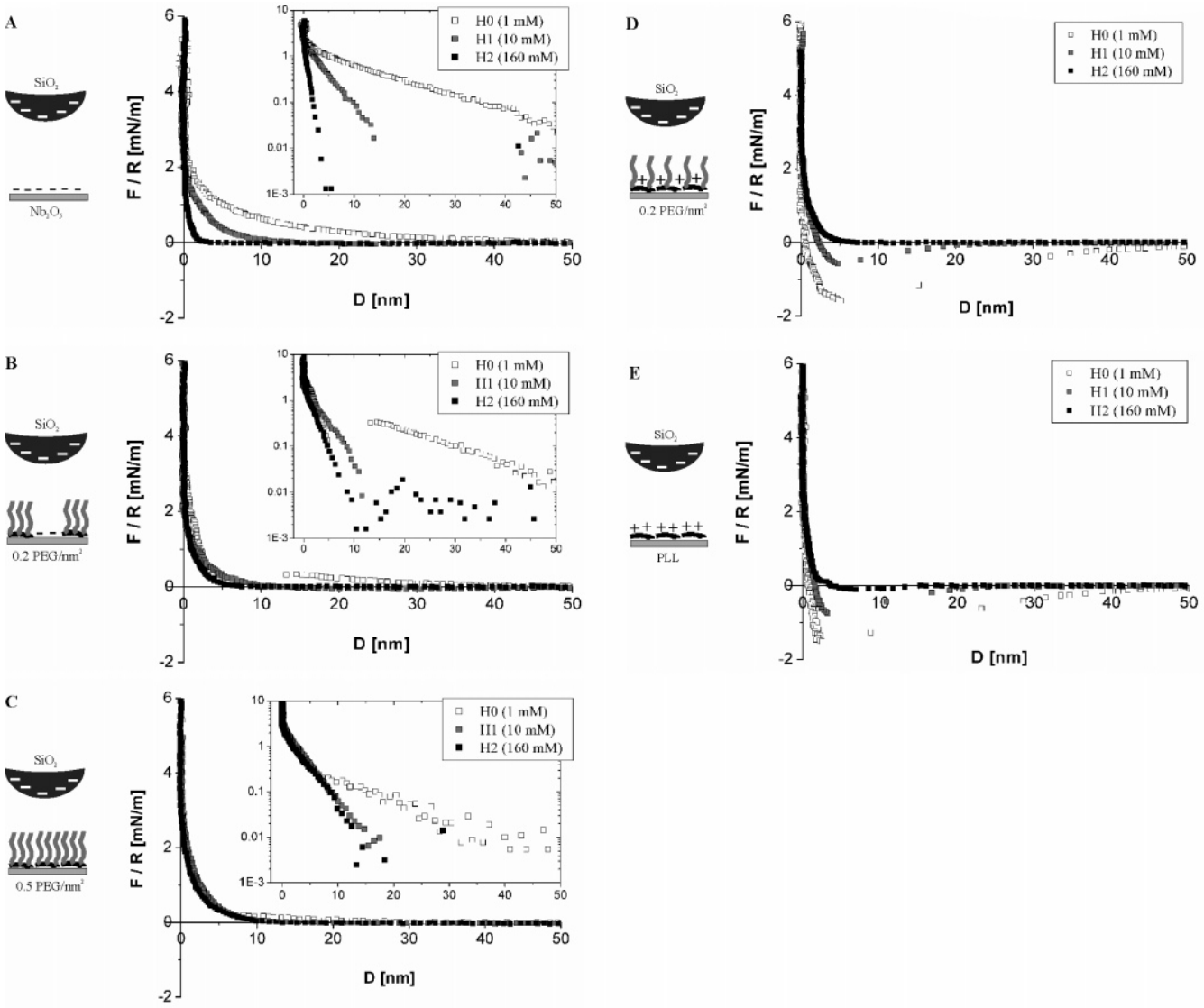

Figure 3. AFM force−distance curves between a negatively charged 4−5 μm SiO_2 microsphere probe and the following surfaces: (A) uncoated Nb_2O_5 substrate, (B) PLL(20)-*g*[3.5]-PEG(2) (1/2), (C) PLL(20)-*g*[3.5]-PEG(2), (D) PLL(20)-*g*[10.1]-PEG(2), and (E) PLL(20) adlayers on Nb_2O_5. From part A to part E, the surface charge gradually changes from negative to positive; the PEG surface density varies from 0 (A and E) to a maximum of 0.5 nm^{-2} (C). The force curves shown were determined in buffer solutions of three ionic strengths, 1, 10, and 160 mM (H0, H1, and H2). All measurements were performed at pH 7.4.

PLL-*g*-PEG-coated surfaces, as shown in Figure 3B−D. In view of the inherent interdependence between the PEG surface density/thickness and the surface charge for the chosen polymeric system, we explore the influence of the PEG layer thickness by varying the thickness of the diffuse ion layer (ionic strength). For the PLL-*g*-PEG surfaces, the measured interaction reflects both an electrostatic contribution and a steric repulsion. The steric repulsion is associated with the PEG side chains, while the electrostatic term arises from the remaining surface charge, where the initial negative charge of the Nb_2O_5 substrate is under- or overcompensated by the adsorbed polycationic polymer. As the ionic strength is associated with the thickness of the diffuse ion layer, the charge of the surface will only be perceptible from a certain distance to the surface. Therefore, the PEG layer shields the surface charge as long as the thickness of the PEG layer exceeds the effective distance of the electrical double layer force. The Debye lengths are ~10, ~3 and <1 nm for the 1, 10, and 160 mM buffer solutions, respectively. As there exists a diffuse ion layer on both the surface and the sphere, the minimum thickness of a PEG layer required to sufficiently screen the surface charges can be 2−3 times the Debye length. The graph of Figure 3C shows the force between the SiO_2 microsphere and the PLL(20)-*g*[3.5]-PEG(2)-coated Nb_2O_5, clearly illustrating the influence of the ionic strength. While similar forces in 10 mM and in 160 mM solutions are indicative of a purely steric repulsive interaction, the force measured in 1 mM solution exhibits two regimes. As the sphere approaches the surface, the net force at first is dominated by a distance dependence (slope) characteristic of the decay length of a repulsive electrostatic force in this medium, then shows a sharp transition to a stronger repulsion at the first contact with the PEG layer, i.e., at the onset of steric repulsion, thus providing information on the thickness of the layer. The sample with a half-monolayer coverage of PLL(20)-*g*[3.5]-PEG(2) shows an even sharper transition in 1 mM HEPES. The transition is also observed in 10 mM HEPES, however this is less obvious in this case as the decay length of the steric interaction is close to the Debye length. Finally, the PLL(20)-*g*[10.1]-PEG(2) polymer shows electrostatic attraction both in 1 and 10 mM HEPES, indicating that the PEG chains do not sufficiently screen the (positive) surface charge of these surfaces under these conditions.

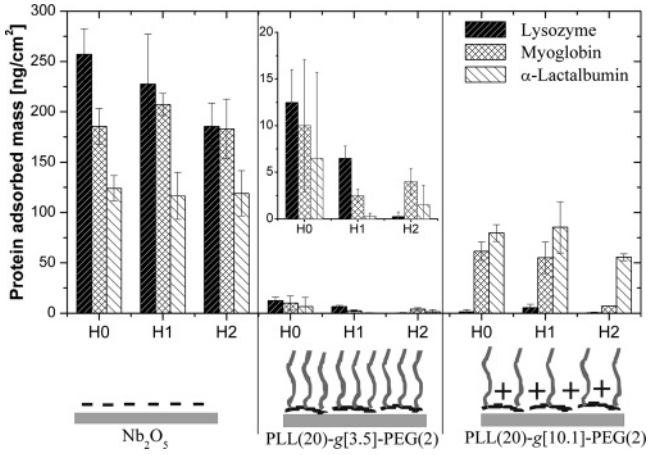

Figure 4. Adsorbed mass of the proteins lysozyme, myoglobin, α-lactalbumin on the five different surfaces, shown schematically in Figure 2, at increasing ionic strengths, measured by OWLS. The ionic strengths were 1 mM HEPES (H0), 10 mM HEPES (H1), and 10 mM HEPES + 150 mM NaCl (H2); all adsorption experiments were performed at pH 7.4.

AFM force measurements thus provide qualitative information on the charge of the different surfaces, as well as on the role of the PEG layer in screening the surface charge to an extent that depends on the ionic strength of the solution. Such measurements are useful as they can provide insight into the potential forces the proteins will sense upon approaching the surface (sections 3.3 and 3.4). For the present purpose, which is to correlate protein adsorption with the nature of the main interfacial forces, quantitative characterization of the forces is not necessary, but detailed analyses of force curves recorded with PLL-*g*-PEG coatings is presented elsewhere.[27]

3.3. Effect of the Ionic Strength on Protein Adsorption. The surfaces were exposed to three different proteins of similar size and shape, but carrying a different net charge at pH 7.4. Lysozyme (IEP 11.1), myoglobin (IEP 7.0), and α-lactalbumin (IEP 4.3) carry a positive, neutral, and negative overall charge, respectively (see Table 1). The adsorption of these proteins onto three surfaces was studied as a function of the ionic strength of the solution, to extract the electrostatic contribution to the interfacial interaction force between proteins and these surfaces. Protein adsorption at a charged surface involves overlap of the electrical double layers at the solvated substrate surface and the solvated protein surface. Figure 4 shows the protein adsorbed mass of the three proteins on uncoated, PLL(20)-*g*[3.5]-PEG(2)- and PLL(20)-*g*[10.1]-PEG(2)-coated Nb_2O_5, measured with OWLS at three ionic strengths, from 1 mM HEPES (H0) to 10 mM HEPES with 150 mM NaCl (H2), lowering the Debye length from ∼10 nm down to <1 nm.

The adsorption of positively charged lysozyme onto Nb_2O_5 showed a dependence on the ionic strength, typical for an electrostatically dominated interaction, with protein adsorbed mass decreasing as the ionic strength increases.[43,44] Myoglobin and α-lactalbumin adsorbed in lesser amounts onto Nb_2O_5, and the adsorbed mass was independent of the ionic strength of the solution. This indicates that other mechanisms were responsible for the observed adsorption of these proteins, possibly accompanied by partial unfolding of the proteins at the interface.[45] The lower adsorbed mass of α-lactalbumin may be attributed in part to the effect of the net negative charge present on both protein and substrate. On the other hand, strong deformation of this soft protein upon adsorption would be expected to increase the footprint of the adsorbed protein, thus decreasing the number of protein molecules per unit area that can be accommodated on the surface.

The adsorption of all three proteins onto PLL(20)-*g*[3.5]-PEG(2)-coated Nb_2O_5 was significantly reduced in comparison to the corresponding behavior on the bare Nb_2O_5 surface (95−100% reduction in protein adsorption). This surface exhibits a dense PEG coating and only a very small negative charge is sensed at the lowest ionic strength (Table 2 and section 3.2).[20] However, a closer look (zoomed inset in Figure 3) reveals an influence of the ionic strength on the adsorption of the "hard" and positively charged lysozyme:[28] protein adsorption decreases with increasing ionic strength. The latter is associated with a diffuse ion layer of defined thickness, described by the Debye length. The influence of the ionic strength on protein adsorption demonstrates the role of PEG layer thickness in shielding the surface charge and thereby preventing strong electrostatic interaction between the surface and the protein. The minimal PEG thickness needed to hide the diffuse ion layer depends on the ionic strength of the solution.

While the positively charged PLL(20)-*g*[10.1]-PEG(2)-coated Nb_2O_5 surface did not adsorb a significant amount of positively charged lysozyme, due to a strong electrostatic repulsive force, the adsorption of myoglobin and α-lactalbumin decreased with increasing ionic strength, illustrating, as for the PLL(20)-*g*[3.5]-PEG(2) polymer, the interplay between the thickness of the polymer layer and that of the diffuse ion layer.

While for small proteins that can penetrate into the PEG layer (primary adsorption) the ionic strength is likely to have only a minor effect on the adsorbed mass, secondary adsorption on top of the polymer layer is expected to be highest at the lowest ionic strengths.[43] As a consequence, general resistance to protein adsorption requires the elimination of both primary and secondary adsorption. Reduction of primary adsorption is achieved primarily through the presence of a dense PEG brush, while secondary adsorption onto PEG graft layers on charged solid substrates due to electrostatic attraction of oppositely charged proteins can be reduced by charge neutralization at the interface and/or sufficiently thick PEG layers that screen the substrate interfacial charge.

3.4. Effect of the Surface Chemistry. To investigate the effects of the surface charge and chemistry on protein adsorption we chose a medium ionic strength with a 10 mM HEPES buffer solution ($\kappa^{-1} \sim 3$ nm), allowing better visualization of the electrostatic interactions compared to physiological conditions (∼150 mM). At 10 mM ionic strength, the PLL(20)-*g*-[3.5]-PEG(2) surface was the only one *not* to display any charge in the colloid probe AFM measurements. The adsorbed mass values for the three proteins are presented in Figure 5 for five surfaces carrying different charges and PEG surface densities (Figure 2).

The surface properties significantly influenced the adsorption of the different proteins. To better discriminate between the effect of surface charge and PEG surface density, surfaces with both negative and positive charge at PEG densities of both 0 and 0.2 PEG/nm^2 were prepared as described in section 2.3 and 2.5 and exposed to the individual protein solutions. Again, as on the other surfaces, lysozyme adsorption showed a pronounced and systematic dependence on the surface charge, only adsorbing onto the negatively charged surfaces. This indicates a dominant electrostatic character of the interaction, as also demonstrated by the influence of the ionic strength (Figure 4). Lysozyme behaves in this respect similarly to a hard colloid particle. Indeed, lysozyme has been reported to be a stable protein that shows comparatively little tendency to lose its native conforma-

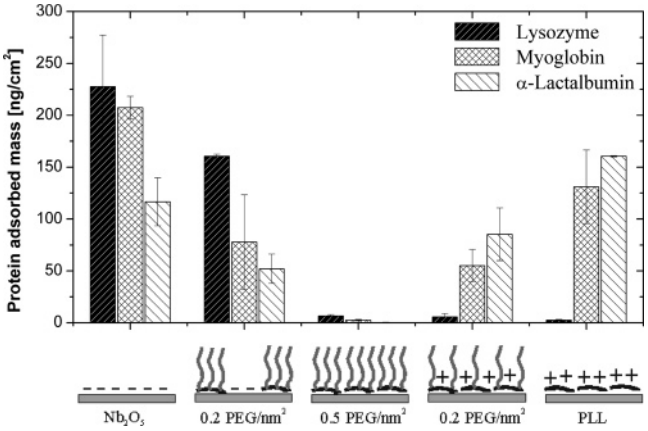

Figure 5. Protein adsorbed mass measured in 10 mM HEPES buffer (pH 7.4) by OWLS, on the five surfaces with various surface charges and PEG surface densities as shown schematically in Figure 2. From left to right the surface charge gradually changes from negative to positive; the PEG surface density passes through a maximum of 0.5 PEG/nm^2 for the PLL(20)-*g*[3.5]-PEG(2) polymer adlayer shown in the middle. Surfaces with a medium value for the average PEG surface density of 0.2 PEG/nm^2 were obtained with PLL(20)-*g*[3.5]-PEG(2) (1/2, i.e., half monolayer coverage), charged negatively, and a monolayer of PLL(20)-*g*[10.1]-PEG(2), charged positively.

tion.[28] In conclusion, controlling the adsorption of hard, charged proteins such as lysozyme therefore simply requires tuning of the surface charge.

The softer protein α-lactalbumin, on the other hand, showed a more complex response. While the adsorbed protein mass slightly increased as the surface became more positive, this overall negatively charged protein adsorbed in significant amounts also on the negatively charged bare (A in Figure 2) and PEG-coated (B) Nb_2O_5, independent of the ionic strength, indicating either the presence of other interaction mechanisms, deformation/unfolding of the protein upon adsorption, or a combination of both. While the overall negatively charged α-lactalbumin could bind with its local positive patches to the surface through electrostatic interaction, other driving forces for protein adsorption are likely be operative in this case including hydrophobic and entropic factors.[28] Indeed, α-lactalbumin has been shown to undergo conformational changes, going through a transition state characterized as "molten globule".[45] Therefore, the adsorption of soft, conformationally delicate proteins such as α-lactalbumin is much more complex and cannot be predicted based on a simple electrostatic model. The adsorbed mass data for the different surfaces suggest that elimination of the adsorption of a soft and "unpredictable" protein such as α-lactalbumin requires complete screening of electrostatic interactions with the underlying substrate by a sufficiently thick PEG layer as well as a repulsive regime exerted by densely packed PEG chains. Both criteria are met for the dense-brushed PLL(20)-*g*[3.5]-PEG(2) layer, the only surface among those tested in this work that resists adsorption of both lysozyme and the other proteins.

The adsorption of neutral myoglobin is mainly controlled by the PEG surface density. Independent of the surface charge, myoglobin adsorbs on surfaces to an extent that is inversely correlated with the PEG surface density (in the regime 0−0.2 nm^{-2}), the surface with the highest PEG surface density (0.5 nm^{-2}) preventing its adsorption almost completely.

In summary, the findings of this study are in general agreement with the conclusions from many other published studies regarding the mechanisms behind the protein resistance of PEGylated surfaces. Electrostatic interactions are clearly found to be important, and dominant in the case of lysozyme. As most proteins do not behave like the "hard" lysozyme, neutralization of the surface charge alone is not sufficient, however, to eliminate protein adsorption in general. Protein resistance is achieved by a combination of several effects: surface charge, surface energy, interfacial water structure, and, in the case of PEGylated surfaces, PEG layer thickness and PEG surface density. Charge neutralization is always effective in eliminating electrostatic interactions between a protein and the surface, but this is not always feasible; most interfaces in contact with aqueous media carry some surface charge. Sufficiently thick PEG layers are therefore needed in order to facilitate the screening of the interfacial charge, thus preventing (bio)-molecules from adsorbing on top of the polymer layer via electrical double layer forces transmitted through the PEG layer. Furthermore, dense PEG layers are essential as a steric barrier to diffusion of the protein between the PEG chains and subsequent adsorption onto the underlying substrate. In addition, the predominantly hydrophilic character of the PEG chains renders the formation of strong hydrophobic forces unlikely, and dense PEG brushes have the particular ability to act as a scaffold for structural water that prevents molecules from permanently interacting with the PEG layer.[46] Finally, the highly mobile and dynamic PEG chains are likely to resist the compression by large protein molecules as a consequence of steric-osmotic effects. Thus, all three modes of adsorption proposed in theoretical work (primary adsorption, secondary adsorption, and the compressive mechanism)[12] can be eliminated with a sufficiently thick, dense PEG layer.

An interesting outcome of this study is, however, that even for the best of the PLL-*g*-PEG coating, which resists protein adsorption under the physiological conditions of 150 mM ionic strength, protein adsorption can be observed as the ionic strength is lowered. Thus, a "nonfouling" coating can become fouling under some solution conditions, due to secondary, electrostatically induced adsorption onto the PEG layer. While an ionic strength of 1 mM is not relevant to biomedical implants, it may be important in some diagnostic applications to consider the possibility of protein/surface interactions arising from electrical double layer forces whose range exceeds the thickness of the repulsive PEG layer under the solution conditions applicable. This insight suggests that the length/molecular weight of the grafted PEG side chains should be tailored such as to match the dimensional requirements imposed by the electrical double layer force, defined by the ionic strength of the intended solution environment.

4. Conclusions

Five model surfaces with different surface charges and quantitatively controlled PEG surface densities were produced using PLL-*g*-PEG polymer adlayers on Nb_2O_5 substrates. Characterization of the surfaces with colloid probe AFM provided information on the surface charge and demonstrated the important role of PEG-layer thickness in shielding the electrical double layer forces. Although it is clear that a hard SiO_2 microsphere does not exactly mimic a soft, nanometer-sized protein, the colloid-probe AFM technique is nevertheless considered to be an excellent tool for independently sensing electrostatic and steric-repulsive forces, by means of ionic-strength variation. Both forces are important in biomolecule-surface interactions. While this approach clearly provides information that is laterally averaged over an area much larger than the size of a protein, and is therefore not sensitive to very local inhomogeneities such as nanodefects in coatings, the

technique provides useful information on the interplay between averaged surface forces and overall levels of protein adsorption. Its usefulness is demonstrated in this study by the close correlation of observed surface forces with measured protein adsorption.

Adsorption of three small model proteins at different ionic strengths on the five types of surfaces revealed the importance of electrostatic forces in protein adsorption. Lysozyme behaved similarly to a hard, positively charged particle, being attracted and repelled by negatively and positively charged surfaces, respectively, but this "simple" behavior is probably rather the exception than the rule.

Myoglobin and α-lactalbumin showed a more complex interaction pattern with the same type of surfaces, likely a consequence of being rather soft proteins, exhibiting changes in conformation upon adsorption. Independent information on the influence of surface charge and PEG surface density highlighted major requirements that PEG graft layers have to fulfill in order to resist adsorption of proteins. While control of the surface charge is sufficient to prevent the adsorption of lysozyme, charge screening with a sufficiently thick and dense PEG layer (min 0.5 PEG (2 kDa) or 25 EG monomers per nm^2) is further needed for most other proteins, including those in serum.[20] Such a PEG layer is able to reduce or eliminate secondary adsorption on the top of the PEG layer, while a high PEG density (brush) is required to prevent primary adsorption by proteins diffusing through the layer and adsorbing onto the underlying surface. Finally, dense PEG chains in a brush conformation provide an entropic insurance preventing proteins from compressing the layer.

Acknowledgment. The authors thank Dr. Graeme Gillies and Dr. Fabiano Assi for assistance with AFM measurements, Michael Horrisberger for performing the niobium oxide coating, and Dr. Oleg Borisov for valuable discussions. This work was financially supported by EPF Lausanne and ETH Zürich (Project TH-33/01-3), the Swiss National Science Foundation, National Research Program NRP 47 (Project No 4047-057548), and by the University of South Australia under the ARC Grant Special Research Centre for Particle and Material Interfaces.

References and Notes

(1) Ratner, B. D. *J. Biomed. Mater. Res.* **1993**, *27*, 837−850.
(2) Ostuni, E.; Chapman, R. G.; Holmlin, R. E.; Takayama, S.; Whitesides, G. M. *Langmuir* **2001**, *17*, 5605−5620.
(3) Schneider, B. H.; Dickinson, E. L.; Vach, M. D.; Hoijer, J. V.; Howard, L. V. *Biosensors Bioelectron.* **2000**, *15*, 13−22.
(4) Norde, W. In *Biopolymers at Interfaces*; Malmsten, M., Ed.; Surfactant Science Series: Marcel Dekker: New York, 1998; Vol. 75.
(5) Norde, W. *Colloids and Interfaces in Life Sciences*; Marcel Dekker: New York, 2003.
(6) Malmsten, M. *J. Colloid Interface Sci.* **1998**, *207*, 186−199.
(7) Leckband, D.; Sheth, S.; Halperin, A. *J. Biomater. Sci.—Polym. Ed.* **1999**, *10*, 1125−1147.
(8) Jeon, S. I.; Andrade, J. D. *J. Colloid Interface Sci.* **1991**, *142*, 159−166.
(9) Jeon, S. I.; Lee, J. H.; Andrade, J. D.; de Gennes, P. G. *J. Colloid Interface Sci.* **1991**, *142*, 149−158.
(10) Szleifer, I. *Biophys. J.* **1997**, *72*, 595−612.
(11) Szleifer, I. *Physica A* **1997**, *244*, 370−388.
(12) Halperin, A. *Langmuir* **1999**, *15*, 2525−2533.
(13) Vermette, P.; Meagher, L. *Colloids Surf. B—Biointerfaces* **2003**, *28*, 153−198.
(14) Morra, M. *J. Biomater. Sci.—Polym. Ed.* **2000**, *11*, 547−569.
(15) Kingshott, P.; Griesser, H. J. *Curr. Opin. Solid State Mater. Sci.* **1999**, *4*, 403−412.
(16) McPherson, T.; Kidane, A.; Szleifer, I.; Park, K. *Langmuir* **1998**, *14*, 176−186.
(17) Efremova, N. V.; Sheth, S. R.; Leckband, D. E. *Langmuir* **2001**, *17*, 7628−7636.
(18) Malmsten, M.; Emoto, K.; Van Alstine, J. M. *J. Colloid Interface Sci.* **1998**, *202*, 507−517.
(19) Lin, Y. S.; Hlady, V.; Gölander, C. G. *Colloids Surf. B: Biointerfaces* **1994**, *3*, 49−62.
(20) Pasche, S.; De Paul, S. M.; Vörös, J.; Spencer, N. D.; Textor, M. *Langmuir* **2003**, *19*, 9216−9225.
(21) Feldman, K.; Hähner, G.; Spencer, N. D.; Harder, P.; Grunze, M. *J. Am. Chem. Soc.* **1999**, *121*, 10134−10141.
(22) Prime, K. L.; Whitesides, G. M. *J. Am. Chem. Soc.* **1993**, *115*, 10714−10721.
(23) Harder, P.; Grunze, M.; Dahint, R.; Whitesides, G. M.; Laibinis, P. E. *J. Phys. Chem. B* **1998**, *102*, 426−436.
(24) Kenausis, G. L.; Vörös, J.; Elbert, D. L.; Huang, N. P.; Hofer, R.; Ruiz-Taylor, L.; Textor, M.; Hubbell, J. A.; Spencer, N. D. *J. Phys. Chem. B* **2000**, *104*, 3298−3309.
(25) Huang, N. P.; Vörös, J.; De Paul, S. M.; Textor, M.; Spencer, N. D. *Langmuir* **2002**, *18*, 220−230.
(26) Elbert, D. L.; Hubbell, J. A. *Chem. Biol.* **1998**, *5*, 177−183.
(27) Pasche, S.; Textor, M.; Meagher, L.; Spencer, N. D.; Griesser, H. J. *Langmuir* **2005**, *21*. 6508−6520.
(28) Arai, T.; Norde, W. *Colloids Surf.* **1990**, *51*, 1−15.
(29) Berman, H. M.; Westbrook, J.; Zeng, Z.; Gilliland, G.; Bhat, T. N.; Weissig, H.; Shindyalov, I. N.; Bourne, P. E. *Nucleic Acids Res.* **2000**, *28*, 235−242.
(30) Huang, N. P.; Michel, R.; Vörös, J.; Textor, M.; Hofer, R.; Rossi, A.; Elbert, D. L.; Hubbell, J. A.; Spencer, N. D. *Langmuir* **2001**, *17*, 489−498.
(31) Ducker, W. A.; Senden, T. J.; Pashley, R. M. *Nature (London)* **1991**, *353*, 239−241.
(32) Ducker, W. A.; Senden, T. J.; Pashley, R. M. *Langmuir* **1992**, *8*, 1831−1836.
(33) Luckham, P. F.; Costello, B. A. D. *Adv. Colloid Interface Sci.* **1993**, *44*, 183−240.
(34) Meagher, L. *J. Colloid Interface Sci.* **1992**, *152*, 293.
(35) Hartley, P. G. In *Colloid-Polymer Interactions: From Fundamentals to Practice*; Farinato, R. S., Dubin, P. L., Eds.; John Wiley & Sons: New York, 1999; pp 253−286.
(36) Israelachvili, J. *Intermolecular & Surface Forces*, 2nd ed.; Academic Press: San Diego, CA, 1992.
(37) Seog, J.; Dean, D.; Plaas, A. H. K.; Wong-Palms, S.; Grodzinsky, A. J.; Ortiz, C. *Macromolecules* **2002**, *35*, 5601−5615.
(38) Vörös, J.; Ramsden, J. J.; Csucs, G.; Szendrő, I.; De Paul, S. M.; Textor, M.; Spencer, N. D. *Biomaterials* **2002**, *23*, 3699−3710.
(39) Kurrat, R.; Textor, M.; Ramsden, J. J.; Böni, P.; Spencer, N. D. *Rev. Sci. Instrum.* **1997**, *68*, 2172−2176.
(40) Höök, F.; Vörös, J.; Rodahl, M.; Kurrat, R.; Böni, P.; Ramsden, J. J.; Textor, M.; Spencer, N. D.; Tengvall, P.; Gold, J.; Kasemo, B. *Colloids Surf. B—Biointerfaces* **2002**, *24*, 155−170.
(41) de Feijer, J. A.; Benjamins, J.; Veer, F. A. *Biopolymers* **1978**, *17*, 1759−1772.
(42) Horbett, T. A. In *Biomaterials Science: An Introduction to Materials in Medicine*; Ratner, B. D., Hoffman, A. S., Schoen, F. J., Lemons, J. E., Eds.; Academic Press: New York, 1996; p 133.
(43) Carignano, M. A.; Szleifer, I. *Mol. Phys.* **2002**, *100*, 2993−3003.
(44) Su, T. J.; Lu, J. R.; Thomas, R. K.; Cui, Z. F.; Penfold, J. *J. Colloid Interface Sci.* **1998**, *203*, 419−429.
(45) Fink, A. L. In *Encyclopedia of Life Sciences*; Nature Publishing Group: London, 2001; http://www.els.net/.
(46) Heuberger, M.; Drobek, T.; Vörös, J. *Langmuir* **2004**, *20*, 9445−9448.